

Charge-density-wave STM observation in η -Mo₄O₁₁

P. Mallet,* H. Guyot, and J. Y. Veuillen
 LEPES-CNRS, Boîte Postale 166, 38042 Grenoble Cédex 9, France

N. Motta

INFM, Dipartimento di Fisica, Università di Roma Tor Vergata, Via della Ricerca Scientifica 1, 00133 Roma, Italy

(Received 11 September 2000; published 5 April 2001)

We present scanning tunneling microscopy (STM) measurements of the two-dimensional η -Mo₄O₁₁ compound, which exhibits Peierls transitions at 30 and 109 K. Using a homemade UHV low-temperature STM, we observe at 50 K (between the two transitions) the formation of an incommensurate charge-density wave (CDW) along the b direction. STM images provide an accurate measurement of the wave vector of this CDW, which is the “nesting” vector characterizing the transition at 109 K. The measured value is in perfect agreement with previous electron diffraction and x-ray diffuse scattering measurements. Finally, recording simultaneously STM images at positive and negative sample bias, we observe the expected π phase shift of the CDW, due to a full spatial separation of the occupied and empty electronic states of the CDW.

DOI: 10.1103/PhysRevB.63.165428

PACS number(s): 71.30.+h, 71.45.Lr, 07.79.Cz

I. INTRODUCTION

Low-dimensional systems often exhibit electronic instabilities, such as, for instance, the Peierls transition. This instability has been studied for years in chalcogenide metals^{1,2} by low-temperature (LT) STM, which provides images with atomic resolution of the charge-density wave (CDW) in the direct space. Concerning molybdenum oxides (MoO) metals, STM and AFM measurements at room temperature have been already obtained, giving precious information about the atomic pattern observed in the normal phase.^{3,4} Low-temperature STM/STS were also performed in several MoO systems, but no CDW observation could be done, suggesting the absence of CDW at the sample surface, possibly induced by the surface preparation.^{5,6}

Very recently, we have presented⁷ a STM observation of the CDW in a quasi-two-dimensional (2D) metallic oxide system, the so-called “purple bronze” K_{0.9}Mo₆O₁₇. Because of the high surface reactivity of these materials, such measurements are hardly achievable without ultrahigh vacuum (UHV) conditions, including cleavage of the surface. Our measurements at 50 K have clearly provided a direct observation of the quasicommensurate 2×2 CDW superstructure existing on the surface. Moreover, we have demonstrated a perfect spatial separation between occupied and empty electronic states of the CDW. In a one-dimensional (1D) system, such a contrast reversal is expected because the local densities of states (LDOS) at $E_F \pm \Delta$ (where E_F is the Fermi energy and Δ is the Peierls gap) have a π relative phase shift. We have used the hidden 1D nesting concept proposed by Canadell and Whangbo⁸ to explain the observed CDW contrast reversal in the two-dimensional (2D) K_{0.9}Mo₆O₁₇ system.⁷

In the following we show LT STM images of another Mo oxide: η -Mo₄O₁₁. This system presents quasi-2D electronic properties, and exhibits two Peierls transitions at 30 and 109 K. Although cleavage is more difficult than in the previous system, we find that it is sometimes possible to achieve STM observation of the CDW in this material.

STM experiments undertaken at 50 K (between the two transitions) clearly show an incommensurate CDW along the b axis, whose wave vector has been carefully measured. Because of the particular shape of the Fermi surface, the CDW vector is along one in-plane direction in this phase.⁸ Simultaneous images taken at opposite bias voltages lead to a perfect contrast reversal of the CDW pattern, just as in the case of a pure 1D CDW.

II. THE MOLYBDENUM OXIDE η -Mo₄O₁₁

The structural chemistry of the intermediate molybdenum oxides was described several decades ago in a series of publications by Khilborg.⁹ The η -Mo₄O₁₁ compound belongs to the monoclinic system, with lattice parameters $a = 24.54 \text{ \AA}$, $b = 5.439 \text{ \AA}$, $c = 6.701 \text{ \AA}$, $\beta = 94.28^\circ$. Its structure is composed of layers of MoO₆ octahedra sandwiched between two planes of MoO₄ tetrahedra. The weaker density of bonds is found between the two tetrahedral planes. Therefore it is commonly believed that cleavage occurs between these two planes. The conduction electrons come mainly from the d orbitals of the inner octahedral planes, giving to the system a quasi-2D metallic behavior. Bulk η -Mo₄O₁₁ undergoes at $T_p = 109 \text{ K}$ a Peierls transition,¹⁰ allowed by a strong electron-phonon interaction and by the particular shape of its Fermi surface: this gives origin to an incommensurate CDW along the b axis, with a wave vector $q = 0.23b^*$ as measured by electron diffraction and x-ray diffuse scattering.¹¹ The Fermi surface, calculated some years ago by Whangbo and Canadell,⁸ compares well with these results. Very recently, angle-resolved photoemission spectroscopy has been achieved¹³ on η -Mo₄O₁₁, giving stronger support to the above theoretical calculations. A second transition occurs at 30 K, identified by resistivity¹⁰ and tunneling¹² measurements as a second Peierls transition. This second transition was out of the temperature range accessible to our instrument. Hence we could not study this low-temperature phase.

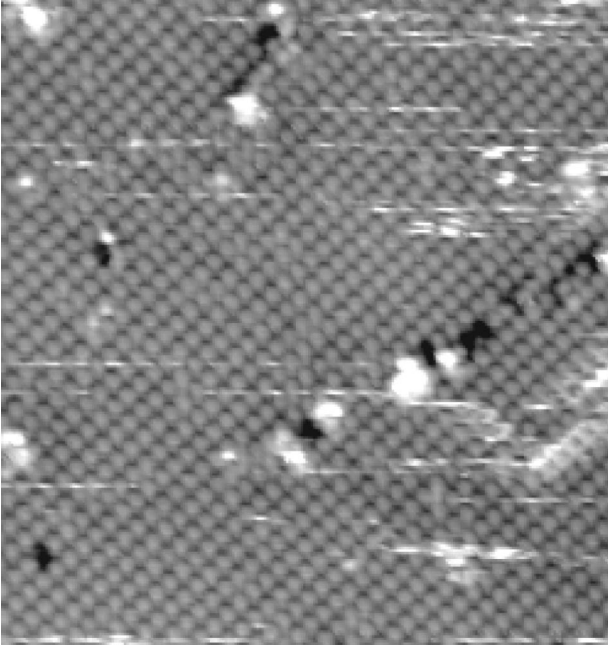


FIG. 1. Empty states image of a cleaved η -Mo₄O₁₁ sample in the normal phase ($T=150$ K). Image size: 20×20 nm². Tunneling current: 0.2 nA. Sample bias: + 0.7 V. The surface lattice parameters measured (by FFT) are $b=5.6$ Å, $c=6.6$ Å. Atomic surface corrugation: 0.7 ± 0.1 Å.

III. EXPERIMENT

STM measurements have been done with a homemade LT STM. The microscope, described elsewhere,⁷ is of Beetle type,¹⁴ and offers the possibility of cooling the sample down to 40 K, together with a very convenient tip or sample exchange procedure. The single crystals were grown by vapor phase transport from a powder, using TeCl₄ as a transport agent.¹⁵ The typical size of the sample is $2\times 2\times 0.5$ mm³. UHV cleavage of the surface is made by pulling off a post glued initially to the surface, by means of a stainless-steel grip. During STM experiment, the base pressure of the chamber is less than 7×10^{-11} mbar, granted by a cryosorption panel cooled by liquid nitrogen. This pump is activated during the experiment in order to minimize the trapping effect of the cooled sample on the residual gases of the UHV chamber.

IV. RESULTS AND DISCUSSION

In Fig. 1 a STM image of the η -Mo₄O₁₁ (100) surface obtained in the normal state ($T=150$ K) is shown, evidencing the rectangular in-plane lattice with corresponding parameters $b=5.6\pm 0.2$ Å and $c=6.6\pm 0.3$ Å. Several defects of atomic size are present, which have a detrimental effect on the tip stability, leading to the unexpected horizontal lines present on the images. The lattice parameters are in good agreement with the literature data,⁹ within the error caused by the small thermal drift in the vertical direction of the image. At this temperature, no CDW pattern is expected, and this is clearly evidenced here.

An important question arises now: is it possible to iden-

tify which atomic plane corresponds to the atomic lattice observed by STM? By considering that the cleavage occurs between the two MoO₄ planes, we expect that the topmost plane of the surface is a MoO₄ tetrahedra plane. This plane is believed to be quite insulating with few electronic states near the Fermi level, while 3d conduction electrons lie in the underneath MoO₆ layers. As a consequence, when the bias is rather low as in Fig. 1 (0.7 V), the tip probes electronic states from the underlying MoO₆ conductive plane, and the electrons have to tunnel through the insulating topmost MoO₄ plane. In such conditions, one may expect to observe the CDW modulation at low temperature.

η -Mo₄O₁₁ is hardly cleavable, and most of our attempts lead to a surface where no CDW pattern could be observed. As an example, the three images presented in Fig. 2, taken at 50 K with different values of bias, do not show any CDW superstructure. Notice that the atomic pattern looks also very disordered, especially on Figs. 2(b) and 2(c) acquired with high bias (1.2 and 2.5 V, respectively). We ascribe the observed pattern on these images to the topmost MoO₄ plane. Certainly due to the unsuccessful cleavage, this plane is very disordered, leading to inhomogeneities in the topographic and electronic structure of the surface. These localized defects dominate the contrast on images 2(b) and 2(c), leading to the disordered pattern observed. Even in Fig. 2(a), taken at low bias (0.25 V), structures correlated with these defects are still observed. They look like fuzzy regions, superimposed to a well-ordered pattern, probably the underneath MoO₆ plane. These regions correspond quite well with atoms of the disordered pattern from Fig. 2(b) (both images are taken at the same location). Unfortunately, these fuzzy regions hide any eventual CDW contrast.

We focus now on the samples for which STM experiments done at 50 K show undoubtedly a CDW pattern. Images are taken at intermediate bias (0.8 V for Fig. 3 and 1 V for Fig. 4). It appears clearly that, contrary to images from Fig. 2, the atomic pattern is well ordered. As the CDW is observed, we believe that the tip probes essentially electronic states of the inner MoO₆ planes. Electronic states confined in the MoO₄ topmost layer must have an energy outside the window fixed by the sample bias, i.e., higher energy than the Fermi level.

At 50 K, below the transition temperature 109 K, a clear modulation along the b axis is observed [Figs. 3(a) and 3(b)]. This modulation is not destroyed neither by small atomic defects nor by the deep trenches (originating from growth defects) present at the surface. By a fast Fourier transform (FFT) analysis of many images [the FFT of Fig. 3(b) is shown in Fig. 3(c)], we recognize extra spots labeled q_{CDW} , featuring in the b^* direction, at the position $q_{CDW}=(0.23\pm 0.01)b^*$. This corresponds to an incommensurate CDW modulation along the b axis. The value of q_{CDW} coincides nicely with satellite positions measured by electron diffraction and x-ray diffuse scattering experiments¹¹ and is also in agreement with the nesting vector found by Fermi-surface calculations.⁸ It is important to remark that although the system has 2D electronic properties, the particular shape of the Fermi surface leads to a CDW characterized by only one direction (b axis) within the plane. Thus, on STM images,

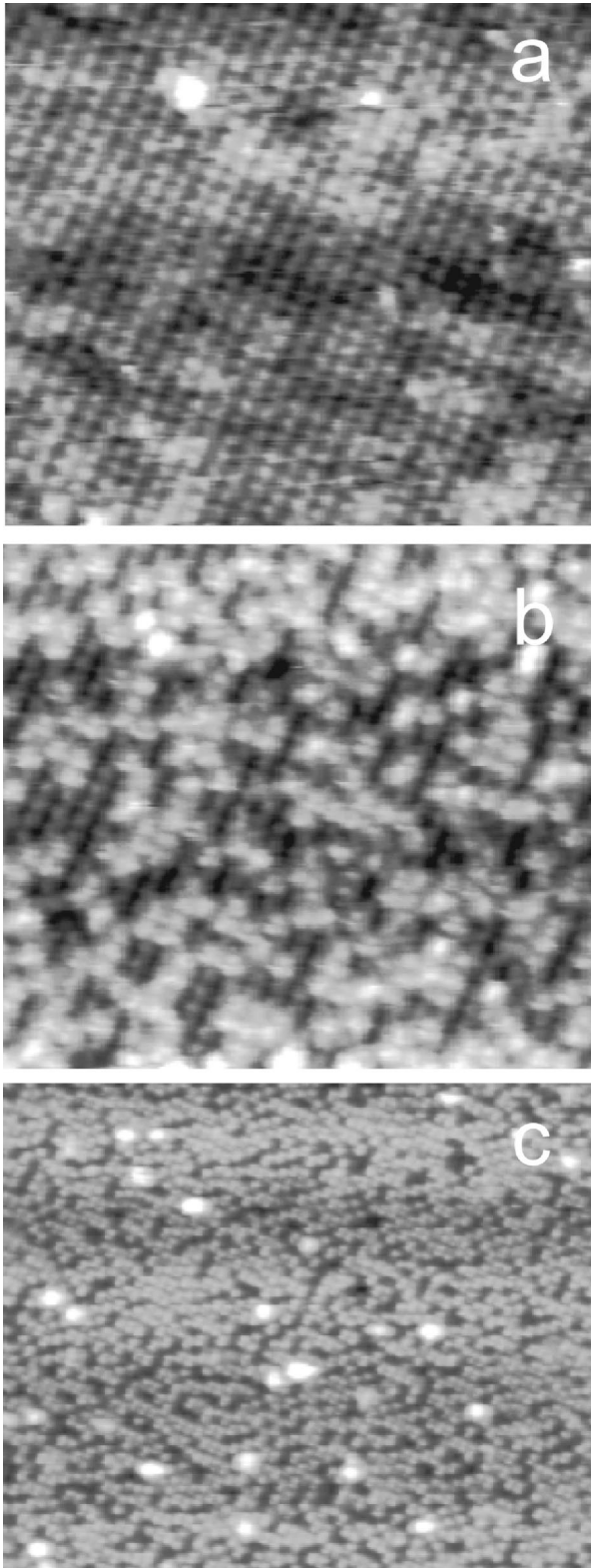


FIG. 2. Low-temperature (50 K) empty states images recorded on a defective cleaved surface. Although temperature is much lower than bulk Peierls temperature (109 K), no CDW pattern is observed. Tunneling current: 0.3 nA, (a) $18.5 \times 16.5 \text{ nm}^2$, sample bias +0.25 V, (b) [same area as (a)] $18.5 \times 16.5 \text{ nm}^2$, sample bias +1.2 V, (c) (same sample, but different region) $43 \times 43 \text{ nm}^2$, sample bias +2.5 V.

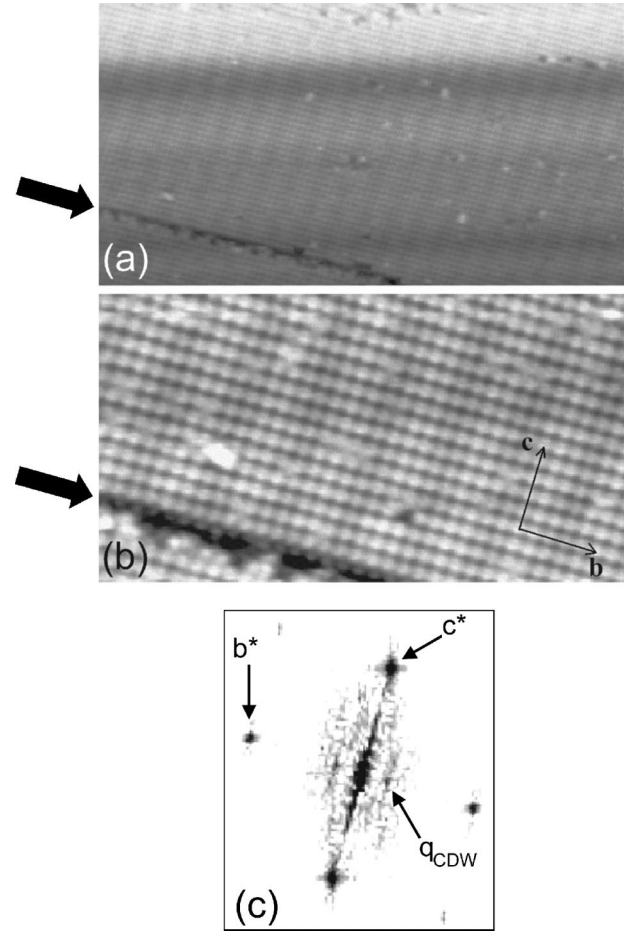


FIG. 3. (a) and (b) Low-temperature (50 K) empty states images recorded on a well-ordered η -Mo₄O₁₁ surface. Image size: $50 \times 27 \text{ nm}^2$ (a), $19.5 \times 11 \text{ nm}^2$ (b). A clear CDW pattern is present on the images, consisting of bands parallel to the c direction, separated by a distance $\sim 4,3 b$. Amplitude of the CDW modulation ($0.2 \pm 0.1 \text{ \AA}$), atomic corrugation ($0.7 \pm 0.1 \text{ \AA}$). Tunneling current: 0.3 nA. Sample bias: 0.8 V. A deep trench, originating from growth defects, is indicated on both images by an arrow. Horizontal bands on (a) are induced by uncontrolled thermal drift. (c) Fast Fourier transform of image (a). Arrows indicate the reciprocal-wave vectors b^* and c^* of the atomic lattice, and the wave vector q_{CDW} of the CDW pattern.

the CDW does not look like a lattice as usually observed in 2D systems, but like parallel bands. The incommensurability of the CDW modulation observed at 50 K is another topic: it confirms the absence of a lock-in transition in η -Mo₄O₁₁, as shown by electron diffraction measurements undertaken at 10 K.¹¹

A very useful feature of the STM is the so-called simultaneous imaging mode at opposite voltage bias, probing at the same location empty and electronic states of the surface. In Figs. 4(a) and 4(b) we show two 50 K STM images of an η -Mo₄O₁₁ surface acquired simultaneously at $V_{\text{bias}} = +1 \text{ V}$ and $V_{\text{bias}} = -1 \text{ V}$. Both images exhibit the CDW pattern, but there is a π phase shift between these two patterns. Because of the small amplitude of the CDW corrugation (0.2 \AA) with respect to the atomic one (0.8 \AA), this effect appears weakly

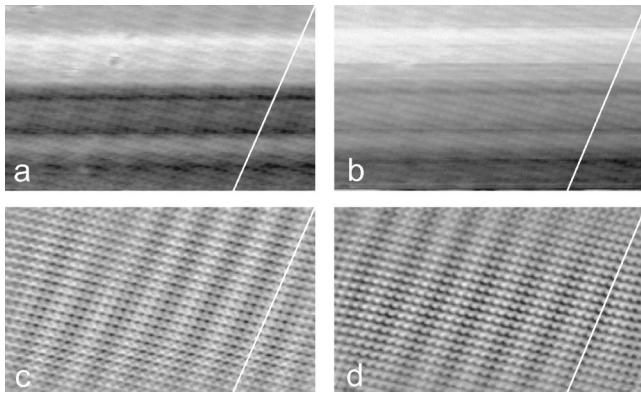


FIG. 4. Occupied (a) and empty (b) states unfiltered images of the same area of the surface, recorded simultaneously. Image size: $20 \times 12 \text{ nm}^2$; tunneling current: 0.3 nA; sample bias: -1 V (a), $+1 \text{ V}$ (b). Horizontal lines are again due to thermal drift and also to probable tip instabilities. To enhance both CDW and atomic arrangements, corresponding filtered data of (a) and (b) are shown, respectively, in (c) and (d), where unexpected frequencies have been suppressed in the 2D FFT spectra. In order to visualize the contrast reversal of the CDW pattern, a white line is drawn exactly at the same location on the four images. The line indicates a maximum (a minimum) of the CDW modulation on occupied (empty) states images.

on rough images, although it really exists. However, using a strong FFT filter, the contrast reversal of the CDW is magnified [Figs. 4(c) and 4(d)]. Referring to the white line drawn exactly at the same location on the images, the maximum amplitude of the CDW on the occupied states image correspond to a minimum on the empty states image. Any FFT artifact has been ruled out, and contrast reversal of the CDW pattern has been observed for several pairs of images.

It is well known^{16,17} that for a 1D atomic chain with one

electron per atom, the Peierls transition opens in the band structure a 2Δ energy gap at the Fermi vector k_F , and that LDOS at energies $E_F + \Delta$ and $E_F - \Delta$, which form the CDW, have a double periodicity with respect to atomic periodicity and have an opposite phase.

Although we deal with a 2D electronic metallic system, the CDW develops in one in-plane direction, and thus the situation is close to the 1D case. STM images taken at a -1 V and $+1 \text{ V}$ probe, respectively, indicate occupied and empty electronic states. A part of these states form the CDW pattern on the images, and we give direct evidence that images of these states have the opposite phase, as expected for a pure 1D atomic chain.

V. CONCLUSION

We present CDW images of $\eta\text{-Mo}_4\text{O}_{11}$. At 50 K an incommensurate modulation along the b direction is observed, well below the Peierls transition. This observation is made difficult because of the quality of the topmost plane, depending on cleavage success. The wave vector of the modulation, which points along the b^* direction, corresponds nicely to that measured by electron and x-ray diffraction. We have also observed the contrast reversal of the CDW between images taken at positive and negative bias, showing the complete spatial separation between occupied and empty electronic states.

ACKNOWLEDGMENTS

We would like to acknowledge Professor C. Schlenker for helpful discussions, G. Fourcaudot for crystal growing, and P. Chevalier for technical assistance. One of us (N.M.) would like to thank the CNRS for financial support and hospitality.

*Corresponding author: Electronic address: mallet@lepes.polycnrs-gre.fr

¹R.V. Coleman, B. Drake, P.K. Hansma, and C.G. Slough, *Phys. Rev. Lett.* **55**, 394 (1985).

²R.V. Coleman, Zhenxi Dai, W.W. McNairy, C.G. Slough, and Chen Wang, in *Scanning Tunneling Microscopy*, edited by J.A. Stroscio and W.J. Kaiser (Academic, San Diego, 1993).

³D. Anselmetti, R. Wiesendanger, H.-J. Güntherodt, and G. Grüner, *Europhys. Lett.* **12**, 241 (1990).

⁴R.L. Smith and G.S. Rohrer, *J. Solid State Chem.* **124**, 104 (1996).

⁵U. Walter, R.E. Thomson, B. Burk, M.F. Crommie, A. Zettl, and J. Clarke, *Phys. Rev. B* **45**, 11 474 (1992).

⁶S. Tanaka, E. Ueda, and M. Sato, *Solid State Commun.* **87**, 877 (1993).

⁷P. Mallet, K.M. Zimmermann, Ph. Chevalier, J. Marcus, and J.Y. Veuilien, *Phys. Rev. B* **60**, 2122 (1999).

⁸E. Canadell and M.H. Whangbo, *Inorg. Chem.* **28**, 1466 (1989).

⁹L. Khilborg, *Ark. Kemi* **21**, 471 (1963); **21**, 357 (1963); **21**, 443 (1963); **21**, 461 (1963); **21**, 365 (1963); *Acta Chem. Scand.* **13**, 954 (1959).

¹⁰H. Guyot, C.E. Filippini, G. Fourcaudot, K. Konaté, and C. Schlenker, *J. Phys. C* **16**, L1227 (1983).

¹¹H. Guyot, C. Schlenker, J.P. Pouget, R. Ayroles, and C. Roucau, *J. Phys. C* **18**, 4427 (1985).

¹²J.P. Sorbier, H. Tortel, C. Schlenker, and H. Guyot, *J. Phys. I* **5**, 221 (1995).

¹³H. Guyot, J. Avila, M.C. Asensio, and G. Fourcaudot (unpublished).

¹⁴K. Besocke, *Surf. Sci.* **181**, 145 (1987).

¹⁵G. Fourcaudot, J. Mercier, and H. Guyot, *J. Cryst. Growth* **66**, 679 (1984).

¹⁶M.H. Whangbo, *J. Chem. Phys.* **73**, 3854 (1980).

¹⁷J. Tersoff, *Phys. Rev. Lett.* **57**, 440 (1986).